Hyperfine Structure of the Metastable Hydrogen Atom*†

JUERGEN W. HEBERLE,‡ HASKELL A. REICH,§ AND P. KUSCH
Columbia Radiation Laboratory, Columbia University, New York, New York

(Received October 7, 1955)

The hyperfine separation $\Delta\nu(2S)$ of the metastable $2^2S_{\frac{1}{2}}$ state has been measured by a new atomic-beam magnetic-resonance method. Rf transitions were detected by utilizing a property peculiar to metastable hydrogen atoms, namely, that atoms with $m_J=-\frac{1}{2}$ decay much more rapidly in passing through a magnetic field of about 575 gauss than do atoms with $m_J=+\frac{1}{2}$. We found that $\Delta\nu(2S)=177\,556.86\pm0.05$ kc/sec. From this result and the very accurately known hyperfine separation $\Delta\nu(1S)$ of the ground state, we obtain $R\equiv\Delta\nu(2S)/\Delta\nu(1S)=\frac{1}{8}$ (1.000 034 6±0.000 000 3). The deviation of R from the presently available theoretical value suggests the existence of a higher-order quantum-electrodynamic term.

A method of velocity selection by electron impact is described.

INTRODUCTION

HERETOFORE, all precise determinations of hyperfine separations by the atomic-beam method were effected by utilizing the deflection of atoms in strongly inhomogeneous fields. This article describes a precise determination of the hyperfine separation $\Delta\nu(2S)$ of the $2\,^2S_{\frac{1}{2}}$ state (hereafter written simply as $2S$) of the hydrogen atom by a new atomic-beam method. Transitions are detected by taking advantage of the fact that in a magnetic field certain magnetic quantum states decay much faster than others.

The hyperfine separation $\Delta\nu(1S)$ of the ground state of the hydrogen atom has been measured by two different methods.[1,2] The theoretical interpretation of those results is hindered by the relatively large uncertainty of the fine-structure constant α. This same difficulty also limits a direct comparison of the observed $\Delta\nu(2S)$ with theory. It is instructive, however, to consider the ratio R defined by $R=\Delta\nu(2S)/\Delta\nu(1S)$. According to the relativistic hfs formulas of Breit[3] this ratio is given by

$$R_{\text{theor}}=\tfrac{1}{8}[1+(\tfrac{5}{8})\alpha^2+0(\alpha^4)]. \quad (1)$$

The deviation from R_{theor} produced by the structure of the proton is expected to be too small to be observable, but quantum-electrodynamic effects of order α^3 may give rise to an observable deviation.

A report[4,5] on our preliminary measurements of $\Delta\nu(2S)$ has been published previously.

GENERAL DISCUSSION

1. Hyperfine Structure of the 2S State

In the absence of a magnetic field a $^2S_{\frac{1}{2}}$ state is split into two levels separated by an energy difference $\Delta W=h\Delta\nu$. The relation of $\Delta\nu(2S)$ to other features of the structure of the hydrogen atom is shown in Fig. 1. In a magnetic field the levels are further split up as described by the Breit-Rabi[6] formula. Most of the discussion by Nafe and Nelson[7] of the transitions between magnetic levels of the ground, $1\,^2S_{\frac{1}{2}}$, state applies also to the $2S$ state of hydrogen.

The Zeeman splitting of the $2S$ and $2^2p_{\frac{1}{2}}$ states is shown in Fig. 2. The symbols α, β, a, b, c, d, e, and f introduced by Lamb and Retherford (HI, p. 560)[8] denote the magnetic levels of the fine structure components of the $n=2$ state. Since we are concerned here with the hyperfine structure of the $2S$ state, we will use the additional notation 1, 2, 3, 4 to designate the magnetic levels of the hyperfine structure, where 1 and 2 are α states and 3 and 4 are β states.

In the presence of weak electrostatic fields, the levels 1, 2, 3, and 4 are shifted in such a way that $\Delta\nu(2S)$ appears diminished. This dc *Stark effect* is discussed in Appendix A.

2. Metastable Hydrogen Atoms

Breit and Teller[9] have estimated that in the absence of perturbing fields the mean lifetime of the $2S$ state lies between 0.11 and 0.16 sec. Upon application of an electrostatic field the $2P$ states are mixed into the $2S$ state, and hence the mean life τ_s of the $2S$ state is reduced. The theory of this electric quenching is given in Appendix II of HI. Such quenching is also produced by the motional electric field $\mathbf{E}=(\mathbf{v}/c)\times\mathbf{H}$ experienced

* Work supported jointly by the Signal Corps, the Office of Naval Research, and the Air Research and Development Command.

† Submitted by Juergen W. Heberle in partial fulfillment of the requirements for the degree of Doctor of Philosophy, in the Faculty of Pure Science, of Columbia University.

‡ Q. W. Boese predoctoral fellow 1953–1954.

§ Present address: Watson Laboratories, New York 27, New York.

[1] J. P. Wittke and R. H. Dicke, Phys. Rev. **96**, 530 (1954).

[2] P. Kusch, Phys. Rev. **100**, 1188 (1955).

[3] G. Breit, Phys. Rev. **35**, 1447 (1930).

[4] Heberle, Reich, and Kusch, Phys. Rev. **98**, 1194 (1955).

[5] Reich, Heberle, and Kusch, Phys. Rev. **98**, 1194 (1955).

[6] G. Breit and I. I. Rabi, Phys. Rev. **38**, 2082 (1931).

[7] J. E. Nafe and E. B. Nelson, Phys. Rev. **73**, 718 (1948).

[8] The articles on the fine structure of the hydrogen atom are referred to as HI, HII, HIII, HIV, HV, and HVI. Those cited in the present paper are HI, W. E. Lamb, Jr., and R. C. Retherford, Phys. Rev. **79**, 549 (1950); HII, W. E. Lamb, Jr., and R. C. Retherford, Phys. Rev. **81**, 222 (1951); HIII, W. E. Lamb, Jr., Phys. Rev. **85**, 259 (1952); HVI, Dayhoff, Triebwasser, and Lamb, Phys. Rev. **89**, 106 (1953).

[9] G. Breit and E. Teller, Astrophys. J. **91**, 215 (1940).

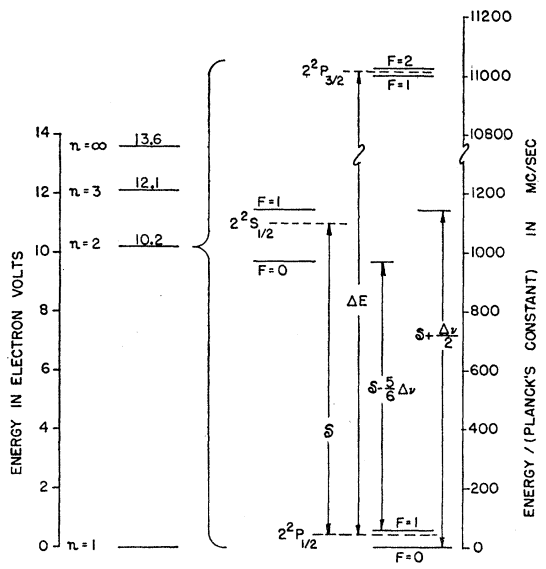

FIG. 1. Energy levels of the hydrogen atom. Lamb shift $=1058 Mc/sec. $\Delta E=10\,968$ Mc/sec.

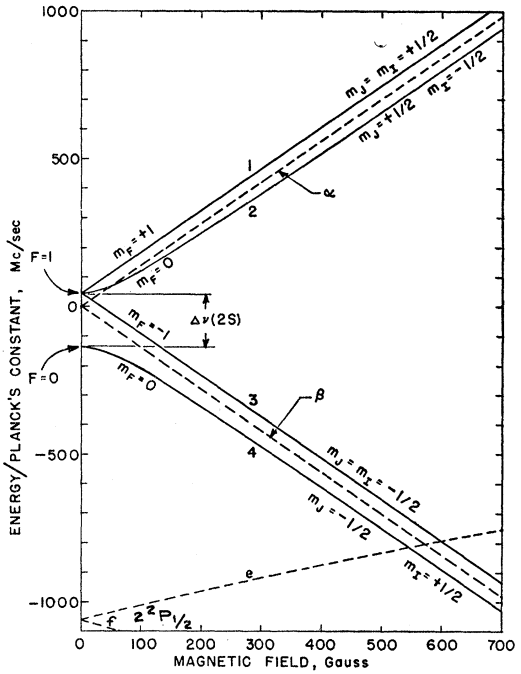

FIG. 2. Zeeman splitting of the hyperfine structure of the 2S state. The dashed lines show the energy levels obtained when hfs is ignored.

by atoms traveling through a magnetic field. The *decay length* λ of a metastable atom is defined by

$$\lambda=v\tau_s. \tag{2}$$

In Fig. 3, the decay lengths of the metastable states α and β have been plotted against H for atoms traveling at a velocity of 5×10^5 cm/sec, which is of the order of magnitude of the velocities occurring in this experiment. The equations from which these curves have been calculated are given in Appendix A. For the β state λ is at a minimum of 0.047 cm at 575 gauss, whereas λ for the α state is as large as 87 cm. It is to be noted that this minimum is associated with the value of H at which the β and e levels cross in Fig. 2.

When a metastable atom impinges upon a metallic surface, its excitation energy ($\sim$10.2 ev) may be transferred to an electron in the metal in such a way that the electron escapes into the vacuum. This phenomenon has been discussed in Sec. 11 of HI. Since atoms in the ground state cannot eject electrons, metastable atoms can be detected and distinguished from normal atoms by collecting these ejected electrons.

METHOD

3. General Description of Method

Of the various transitions allowed between the states 1, 2, 3, and 4 several pairs may be used to determine $\Delta\nu(2S)$; those lines whose observation leads to a determination of $\Delta\nu(2S)$ in the present work are the π line (1,4) and the σ line (2,4). For low H (i.e., $H\ll h\Delta\nu/\mu_0$) their resonant frequencies are given by

$$\nu_{14}=\Delta\nu+AH+BH^2, \tag{3}$$

$$\nu_{24}=\Delta\nu+CH^2, \tag{4}$$

where $A=1\,399.1$ (kc/sec) gauss^{-1}, $B=11.092$ (kc/sec) gauss^{-2}, and $C=2B=22.184$ (kc/sec) gauss^{-2}.

In the computation of B, a value of 177 557 kc/sec was assumed for $\Delta\nu$. It is to be noted that ν_{24} is independent of H in the first order, and the choice of lines used in the present work was motivated by this fact.

The long decay length of the 2S state at weak magnetic fields suggests the adoption of an atomic-beam method for investigating the hyperfine structure of this state. Hydrogen atoms in the ground state are formed by dissociating molecular hydrogen and effuse through a small hole into vacuum. A beam is formed by those atoms that pass through a slit in a nearby bulkhead. The atoms are then excited to the metastable state by electron impact. Thereupon the beam is *polarized*, i.e., atoms in the final state of the transition being observed are quenched selectively. The beam passes next through a radio-frequency magnetic field, where transitions to the final state are induced. Subsequently the beam is subjected to *analysis*, i.e., the newly formed final-state atoms are quenched. The remaining metastable atoms pass on to a detector. A decrease of the detector signal, as the radio-frequency is varied, indicates a resonance. This sequence of processes is illustrated in Fig. 4 and will be discussed in detail in subsequent sections.

4. Dissociation and Excitation

Various methods have been used to dissociate hydrogen for the purpose of forming a beam of hydrogen

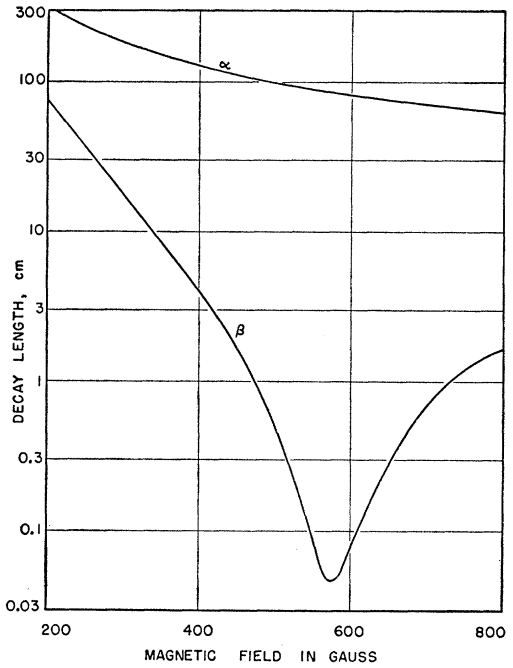

FIG. 3. Decay length as a function of magnetic field for the metastable states α and β at a velocity of 5.0×10^5 cm/sec perpendicular to the magnetic field.

atoms: (1) Wood's tube,[10] (2) microwave discharge,[11] (3) thermal dissociation (HI, Sec. 21; HII, Sec. 34). We decided to use thermal dissociation because of its previous success in the work of Lamb *et al.*[8] Moreover an oven is compact and readily movable within the vacuum system, and recombination in an oven poses much less of a problem than in a discharge tube.

The $2S$ state is most readily excited by electron impact. Conceivably the $2S$ state could also be produced by exciting the $3P$ state optically with Lyman β photons; the $2S$ state would then be populated by spontaneous radiative transitions from the $3P$ state. The latter method, however, is troublesome because it is difficult to obtain a sufficiently high density of Lyman β photons in the excitation region.

5. Polarization and Analysis

Lamb and Retherford (Sec. 16 of HI) have pointed out that a beam of metastable atoms becomes polarized as it traverses a magnetic field corresponding to the βe crossing point; the β atoms are strongly quenched by the motional electric field, and the excited atoms that emerge from such a magnetic field are all in the α states. This process of polarization does not restrict the cross-sectional area of the beam, whereas in the usual atomic-beam experiments the cross section of the beam must be very small in order that the deflection of atoms by inhomogeneous fields may be observed. The phenomenon of differential magnetic quenching can also be employed to effect analysis; only α atoms can traverse an analyzing field of about 575 gauss without being totally quenched. From Fig. 3, it appears that the strength of the polarizing (or analyzing) field is not critical, but that adequate polarization (or analysis) occurs over a considerable range of field strengths.

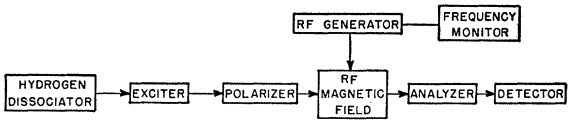

FIG. 4. Block diagram of apparatus.

A radio-frequency method has been suggested by Lamb,[12] for achieving polarization and analysis: Let f_1 be a frequency slightly greater than $S+\frac{1}{2}\Delta\nu$ and f_2 somewhat less than $S-(5/6)\Delta\nu$ (see Fig. 1). By passing metastable atoms through an oscillating electric field of frequency f_1 the atoms in the $F=1$ state are quenched selectively. Alternatively by application of frequency f_2 the $F=0$ state is quenched selectively. By operating the polarizer and analyzer at the same frequency (either f_1 or f_2) a decrease in detector signal is observed consequent to a transition $|\Delta F|=1$ in the region between polarizer and analyzer. On the other hand, if the analyzer and polarizer are operated at different frequencies (the polarizer at f_1 and the analyzer at f_2, or *vice versa*), metastable atoms can reach the detector only if they undergo a transition in the region between the polarizer and analyzer.

For the present work magnetic polarization and analysis was chosen in preference to Lamb's rf method, because the former is technically simpler, and because it is desirable to have a magnetic field of several hundred gauss for focusing the electrons in the exciter.

6. Rf Transitions and Detection

Ramsey's method[13] of separated oscillating fields was chosen for inducing the transitions (1,4) and (2,4). The line width W of the central peak of the resonance pattern is measured at a percentage rf quenching $\phi_W=\frac{1}{2}[\phi_M+\frac{1}{2}(\phi_A+\phi_B)]$, where ϕ_M is the maximum percentage quenching and where ϕ_A and ϕ_B are the values of percentage quenching at the adjacent minima as illustrated on curve *II* of Fig. 5. (See Sec. 14 for the definition of ϕ.) For atoms of uniform velocity v, the line width is given by $W=v/(2L)$ where L is the distance separating the two oscillating fields. If the second oscillating field leads the first by a phase[14] angle δ, the central peak is shifted to a lower frequency by an amount $W\delta/\pi$. The region between the oscillating fields, that is traversed by those metastable atoms which later hit the detector, will be called the *precession region.*

[10] Rabi, Kellogg, and Zacharias, Phys. Rev. **46**, 157 (1934).
[11] Nagle, Julian, and Zacharias, Phys. Rev. **72**, 971 (1947).
[12] W. E. Lamb, Jr. (private communication).
[13] N. F. Ramsey, Phys. Rev. **78**, 695 (1950).
[14] N. F. Ramsey and H. B. Silsbee, Phys. Rev. **84**, 506 (1951).

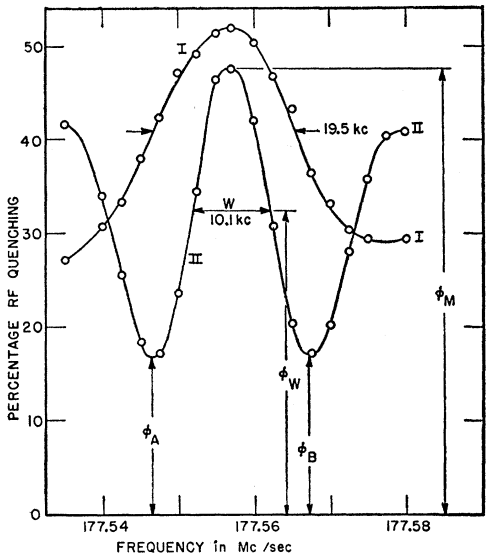

FIG. 5. Two resonance curves illustrating the definition of the line width W and showing the effect of velocity selection upon W.

Two alternative methods of detection are available: (1) collection of electrons ejected from a metal surface by metastable atoms; (2) detection of the Lyman α photons produced when β atoms are quenched in the analyzer. Method (1) suffers from the disadvantage that photons produced in the exciter may also eject electrons thus adding a constant background to the detector signal. As explained in Sec. 9, an *electrostatic quencher* can be employed to distinguish between metastable atoms and photons. Hence the photon background is undesirable only in so far as fluctuations in the photon flux contribute to the noise in the detector signal. Despite this disadvantage method (1) was chosen because of its previous success.[8]

7. Velocity Selection

In most atomic and molecular beams, the number of particles that arrive at the detector in unit time with a velocity within the interval dv is proportional to $v^3 \exp[-Mv^2/(2kT)]dv$, where M is the mass of a particle. In the present experiment, however, the excitation by electron impact effects a velocity selection because the impact, which is directed transverse to the beam, gives different deflections to atoms of different initial velocities. For a given geometry of oven, exciter, and detector, only atoms having undergone a certain small range of deflections by electron impact will reach the detector. Only atoms in a certain range of velocities will fall into this range of deflections. Since the width W of the resonance line is proportional to velocity, it is possible to adjust W within rather wide limits by changing the geometry of the apparatus. A useful purpose is served by selecting slow atoms; as the average velocity of atoms in the beam is reduced, the line width decreases, and it becomes possible to determine the frequency of the line center more accurately.

APPARATUS

8. General Features

Most of the essential features of the apparatus are depicted in Fig. 6. As in all atomic-beam devices in this apparatus, too, the mean free path of atoms in the beam must be at least as long as the beam. Accordingly the vacuum system is divided into three chambers each of which is exhausted separately by a 3-stage fractionating diffusion pump. The *first* chamber contains the dissociator and is pumped at a measured rate of about 400 liters/sec. The relatively small amount of hydrogen introduced into the other two chambers is pumped back into the first chamber. Two liquid-nitrogen traps serve to reduce the oil vapor pressure in the exciter chamber and in the rf region.

The dissociator is a tungsten tube heated by electron bombardment; it will be described in a paper to be submitted for publication in the *Review of Scientific Instruments*. The atoms pass to the exciter E through a slit with vertical, independently adjustable jaws J.

Hydrogen gas was admitted to the dissociator through a Nier[15] leak from a 35-liter brass ballast tank, in which the gas was stored at about 10 psi above atmospheric pressure. Instead of a copper[15] tube our variable leak

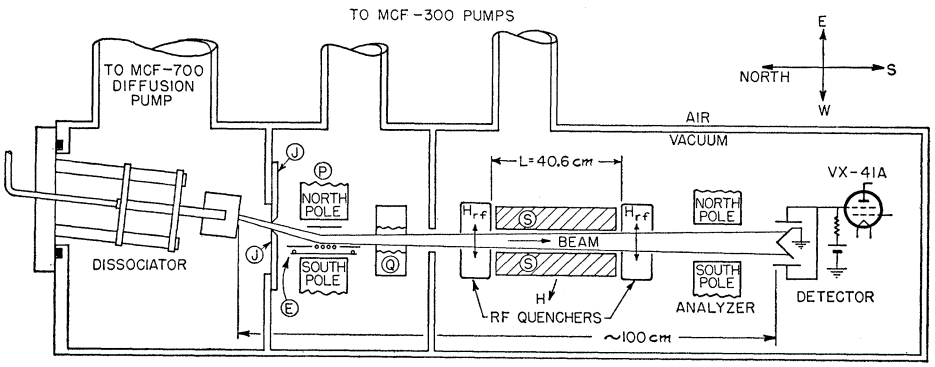

FIG. 6. Schematic plan view of apparatus, not drawn to scale. J, movable slit jaws; E, exciter; P, polarizer; Q, electrostatic quencher; S, heated electrostatic shield. The vector H indicates the direction of the magnetostatic field in the precession region.

[15] Nier, Ney, and Inghram, Rev. Sci. Instr. 18, 191 (1947).

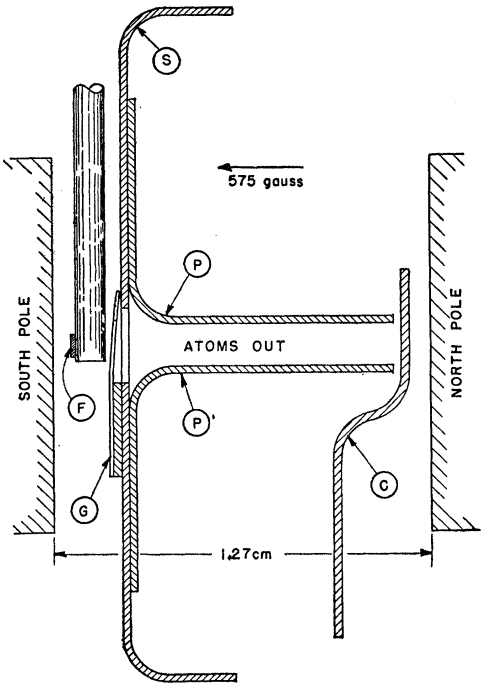

FIG. 7. Cross section through the exciter perpendicular to the atomic beam. *F*, tungsten filament, 0.01×0.12×3.8 cm; *G*, molybdenum grid wires, 0.05 mm diam; *S*, support for grid, molybdenum; *P*, plates for reducing space-charge effects; *C*, electron collector.

contains a flattened tube of stainless steel. In order to remove any residual oxygen which might attack the tungsten oven, the gas was passed through a Deoxo hydrogen purifier and a liquid-nitrogen trap.

9. Exciter, Polarizer, and Electrostatic Quencher

A sectional view of the exciter, which is a modified version of the one described in Sec. 35 of HII, is shown in Fig. 7. The opening in the support *S*, which extends 1.27 cm along the beam direction, is covered by 37 equally spaced grid wires *G* which are held only at one end to prevent buckling. It is important to make the filament long enough so that the temperature is reasonably uniform along the portion opposite the grid. Then the electron current will be uniformly distributed along this length of 1.27 cm, and hence quenching of metastable atoms by space-charge fields is minimized. A substantial increase in the yield of metastable atoms was obtained when the filament-grid separation was increased from about 0.03 cm to 0.15 cm. An excitation voltage of about 13 v dc is applied between the filament and the grid, which is grounded. The collector *C* is connected to ground through a microammeter.

The exciter is located in the gap of a double-yoke electromagnet which serves as a polarizer and focuses the electrons. The gap of the polarizer is 1.27 cm, and the pole-face dimensions are 2.03×1.27 cm.

As explained in Sec. 6, some means of distinguishing between metastable atoms and photons is required. For this purpose, the beam is passed between two parallel horizontal brass plates which constitute an electrostatic quencher (*Q* in Fig. 6). The plates are 1.90 cm long along the beam and separated by 0.635 cm. A potential difference of 20 v dc applied between the plates suffices to quench all metastable atoms in the beam, but of course photons traverse this electric field without being disturbed.

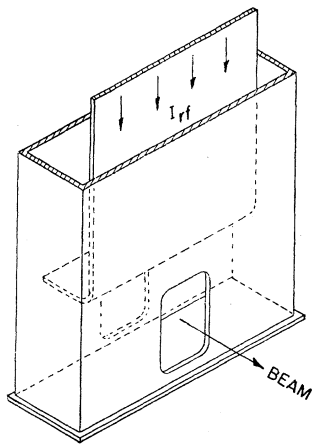

FIG. 8. Rf quencher. The beam passes through two apertures 1.90×2.54 cm.

10. Rf Region

Two rf quenchers of the design shown in Fig. 8 are mounted inside the vacuum envelope separated by a distance $L=40.6$ cm. They have been so designed that the electric field is small in the region traversed by the beam. Connections to each rf quencher are separately brought out through the vacuum envelope and are joined rigidly by a coaxial transmission line. Rf power is supplied at a feed point at the center of the transmission line. The phase angle δ between the two rf magnetic fields would be zero, if the Joule losses on each side of the feed point were equal. Since the structure is symmetric, the losses should be the same on each side. Accidental imperfections in the symmetry, however, give rise to a small phase angle. A General Radio rf voltmeter (type No. 1800-*A*) monitors the rf voltage applied at the feed point.

It can be seen from Eq. (4) that it is advantageous to measure ν_{24} at a low value of H because the derivative $d\nu_{24}/dH$ is proportional to H. Therefore the precision with which H must be determined is reduced markedly as H is decreased. The magnetic field in the precession region is the earth's field as modified by magnetic objects in the vicinity. Since its vertical component is considerably larger than its horizontal component, H can be greatly reduced by canceling the vertical component. This is done by passing an appropriate current through a horizontal rectangular coil of dimensions 51×168 cm. As shown in Fig. 6, the angle between the residual magnetostatic field and H_{rf} is

about 30°. Thus it is possible to induce both π and σ transitions.

In order to reduce stray electrostatic fields in the precession region, this region has been surrounded by a massive shield (S in Fig. 6) of OFHC copper. This *electrostatic shield* can be heated electrically to drive off insulating deposits on which charges might accumulate.

11. Rf Generator and Frequency Measurement

A 32V-3 amateur transmitter[16] is operated in the neighborhood of 29.6 Mc/sec. Its output is multiplied and amplified as indicated in Fig. 9. By powering the transmitter from a Sorensen model 1001 regulator and by warming it up for six hours it was possible to achieve a frequency stability of one part in twenty million over an interval of several minutes. A General Radio interpolation oscillator (type No. 1107-A) was used to compare the frequency of the transmitter with a suitable combination of harmonics and subharmonics of the 100-kc frequency standard of the Molecular Beams Laboratory.

TABLE I. Typical operating conditions.

Gas flow	0.10 cc/sec STP of molecular hydrogen
Pressure in first chamber	3×10^{-4} mm of mercury
Oven bombardment	216 watts
Oven temperature	~2800°K
Excitation voltage	12.8 volts
Excitation current	400 microamperes
Detector currents	
Beam intensity	61 cm on galvanometer scale 5.6×10^{-14} amperes 3.5×10^{5} electrons/sec
Photon background	20 cm on galvanometer scale

12. Analyzer and Detector

In the initial experimentation an electromagnet was used as analyzer. It was found that its current could be changed by about 25 percent without altering the intensity of the π line (1,4) significantly. This observation illustrates our earlier remark (Sec. 5) that the strength of the analyzing field is not critical. When an analyzer with a larger gap was needed, the permanent magnet shown in Fig. 10 was built and used in the final measurements of $\Delta\nu(2S)$.

The detector is essentially the same as that described in HI and HII. The target is made of 0.025-cm molybdenum sheet and presents an area of about 8 cm² to the beam. A Penick[17] circuit amplifies the electron current so that it can be measured with a mirror galvanometer. The Victoreen VX-41A electrometer and its 2×10^{11} ohm input resistor are mounted south of the target inside the vacuum. The current sensitivity of the detector is about 10^{-15} amp/cm, and the time constant is 4 sec.

[16] Manufactured by the Collins Radio Company, Cedar Rapids, Iowa.

[17] D. B. Penick, Rev. Sci. Instr. **6**, 115 (1935).

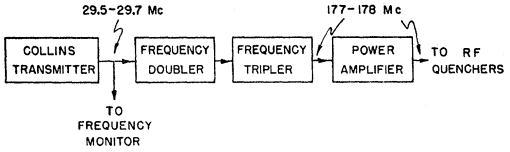

FIG. 9. Block diagram of rf generator.

OBSERVATIONS

13. The Signal

In Table I are given typical values of various parameters describing the performance of the apparatus. The *beam intensity* is obtained by observing the galvanometer deflection when the electrostatic quencher is turned on. It is a measure of the flux of metastable atoms striking the detector target. The background photons originate principally in the exciter (Lyman α radiation) although some are produced by the dissociator. The beam of metastable atoms was produced reliably, and loss of beam occurred only rarely. No poisoning of the exciter, such as was reported in Sec. 28 of HI and in Sec. 43 of HIII, was ever observed. It was never necessary to heat the detector in the manner described in Appendix X of HVI. In fact our detector was not equipped with heaters.

14. Procedure

The entire apparatus was turned on to allow all heated parts to outgas and stabilize. The electrostatic shield was heated until it glowed a dull red; before resonance data were taken, the power was turned off. Because it is massive and well insulated thermally, the shield remained hot for the duration of a run. The frequency standard was adjusted with respect to WWV.

The field-dependent frequency ν_{14} was measured by determining two frequencies ν_a and ν_b on opposite sides of the (1,4) line for which the galvanometer deflection

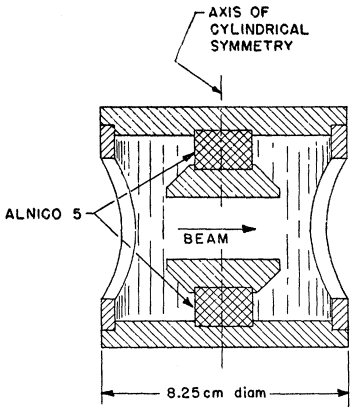

FIG. 10. Permanent magnet used as analyzer. Except for the two slugs of Alnico 5 it is made of cold-rolled steel.

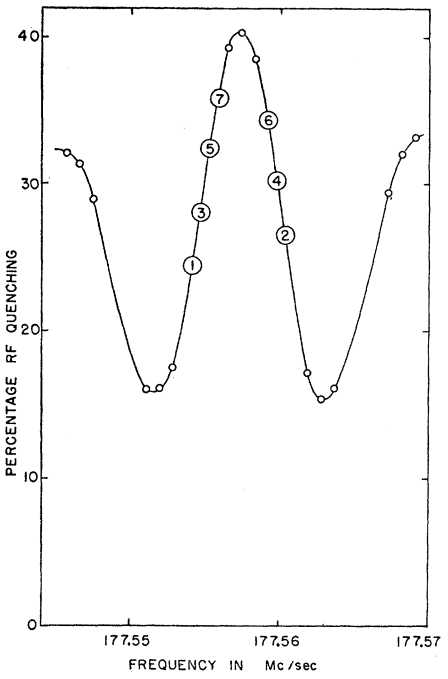

FIG. 11. Experimentally obtained resonance curve for the σ line (2,4). The numbered points are used to determine ν_{24}.

was the same. Then ν_{14} was taken to be the average of ν_a and ν_b.

The frequency ν_{24} was determined by plotting out a resonance curve such as the one shown in Fig. 11. The effect of the rf magnetic fields is measured by reading the galvanometer when the rf voltage is on and when it is off. The difference between the two readings is called the *rf quenching*. The *percentage quenching* ϕ is defined by $\phi=100$ (rf quenching)/(beam intensity).

The percentage quenching is measured at various frequencies and a resonance curve is plotted at constant rf voltage. To reduce errors possibly caused by drift the points labeled 1 to 7 in Fig. 11 were taken in zig-zag fashion in the order of the numerals. The center ν_c of the line is obtained by combining any three consecutive points $n-1$, n, $n+1$ according to the formula

$$\nu_c=\tfrac{1}{2}\{\nu_n+\nu_{n-1}+[(\phi_n-\phi_{n-1})/(\phi_{n+1}-\phi_{n-1})]\times(\nu_{n+1}-\nu_{n-1})\}. \quad (5)$$

The five values of ν_c obtained from a single resonance curve are averaged, and a value of ν_{24} is obtained, as illustrated in Table II. (No significant error is introduced by the assumption contained in Eq. (5) that ϕ varies linearly with ν between the points $n-1$ and $n+1$.) Immediately afterwards ν_{14} is redetermined. The average of the two values of ν_{14} is substituted together with ν_{24} in Eqs. (3) and (4).

The value of $\Delta\nu'$ obtained by solving these equations is primed to indicate that this result is still uncorrected for a phase-shift error (see Sec. 6). Although the rf quenchers were designed to be supplied with rf power symmetrically, imperfections in this symmetry give rise to a phase difference δ between the two rf magnetic fields. The frequency shift produced by δ is reversed by lifting the rf quenching assembly out of the apparatus, turning it end for end, and reinstalling it. This reversal can be accomplished without changing any important electrical connections; thus the sign of δ, and with it the sign of the frequency shift, is changed but not its magnitude. Now $\Delta\nu'$ is redetermined. By averaging two such values of $\Delta\nu'$ the error arising from the phase angle δ is eliminated.

15. Results

At the exploratory stage of this work, resonance data were taken with $L=20$ cm in order to investigate velocity selection. First, the dissociator was placed as far to the west as was consistent with the detection of a usable beam intensity. The resulting resonance curve is shown in Fig. 5 (*I*). The dissociator was then translated eastward by 0.8 cm, and another resonance curve (*II* in Fig. 5) was observed. From the line widths it is clear that it is possible almost to double the average velocity of atoms in the beam simply by changing the deflection angle.

Later L was increased to 40.6 cm, and $\Delta\nu(2S)$ was determined by five traversals of the (2,4) resonance. The result has been reported[5] as $\Delta\nu(2S)=177\,556.6\pm0.3$ kc/sec. Although the statistical uncertainty was of the order of 0.05 kc/sec, a larger uncertainty was quoted because of unknown errors arising from rf Stark effect, dc Stark effect, and phase shift. In fact, the rf quenchers then used had a considerable rf electric field in the region traversed by the beam, as evidence by substantial rf quenching ($\sim$20%) at frequencies far away from resonance.

In order to explore these errors, two new rf quenchers (Fig. 8) and the electrostatic shield were installed.

TABLE II. Sample determination of $\Delta\nu'(2S)$. The values of ν_c were obtained from the resonance curve of Fig. 11.

ν_{14} before traversal of the (2,4) resonance = 177 784.2 kc/sec
$H=0.1625$ gauss $\quad\nu_{24}-\Delta\nu(2S)=0.585$ kc/sec

$n-1$	n	$n+1$	ν_c (kc/sec)
1	2	3	177 557.422
2	3	4	0.428
3	4	5	0.400
4	5	6	0.389
5	6	7	0.417

Average value of ν_c and P.E. = 177 557.411$\pm$0.005 kc/sec = ν_{24}

ν_{14} after traversal of the (2,4) resonance = 177 783.0 kc/sec
$H=0.1615$ gauss $\quad\nu_{24}-\Delta\nu(2S)=0.578$ kc/sec

Average $\nu_{24}-\Delta\nu(2S)=0.582$ kc/sec
$\Delta\nu'(2S)=177\,556.830\pm0.005$ kc/sec

Resonance data were taken under four different conditions:

$A(+)$: without the electrostatic shield, positive phase shift;
$A(-)$: without the electrostatic shield, negative phase shift;
$B(+)$: with the electrostatic shield hot, positive phase shift;
$B(-)$: with the electrostatic shield hot, negative phase shift.

The values of $\Delta\nu'(2S)$ obtained under conditions A are displayed in Fig. 12. The average values are

$$\Delta\nu'(2S)=177\ 556.875\pm0.010 \text{ kc/sec for } A(+),$$
$$\Delta\nu'(2S)=177\ 556.805\pm0.010 \text{ kc/sec for } A(-).$$

By averaging these two results the phase shift is eliminated, and $\Delta\nu(2S)=177\ 556.840\pm0.010$ kc/sec for conditions A. For $B(+)$ we obtained 177 556.885, 177 556.860, and 177 556.890 kc/sec; and for $B(-)$ 177 556.820, 177 556.830, and 177 556.830 kc/sec. So for conditions B

$$\Delta\nu(2S)=177\ 556.850\pm0.010 \text{ kc/sec.}$$

The line width W in these measurements is about 5.5 kc/sec, which corresponds to an average velocity of 4.5×10^5 cm/sec. In spite of the close agreement of the results A and B we use only the latter result in arriving at our final quoted result.

16. Corrections

Systematic errors may arise from (1) rf Stark effect (see Appendix A), (2) dc Stark effect, (3) inhomogeneity of the magnetostatic field in the precession region, (4) overlap of the (1,4) and (2,4) resonances, (5) variation of rf magnetic field with frequency, and (6) frequency standard.

In order to detect an rf Stark effect, $\Delta\nu(2S)$ was measured under conditions $A(+)$ and $A(-)$ at rf voltages of 40, 49, 60, 70, and 80 volts as shown in Fig. 12. No clear-cut effect is discernible, but the results are not inconsistent with the occurrence of a small effect of the magnitude listed in Table III.

TABLE III. Corrections and errors.

	Minimum kc/sec	Maximum kc/sec
rf Stark effect	0	+0.01
dc Stark effect	0	+0.01
Inhomogeneity of magnetic field	−0.01	0
Overlap	−0.01	+0.02
Frequency standard	−0.01	+0.01
	−0.03	+0.05
Statistical error (P.E.)	−0.01	+0.01
	−0.04	+0.06
Total correction and error	+0.01±0.05 kc/sec	

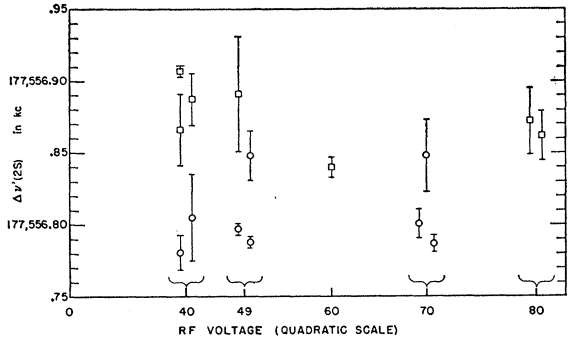

FIG. 12. Experimental values of $\Delta\nu'(2S)$ as a function of rf voltage. The vertical lines represent average deviations. The squares were measured under condition $A(+)$, while the circles were determined under conditions $A(-)$.

The electrostatic shield was provided to eliminate dc Stark effect. In Sec. 15, it appeared that the presence of the hot shield did not affect the result significantly. Nevertheless an allowance for a possible residual effect is made in Table III.

Field inhomogeneity introduces an error because the value of ν_{14} depends upon the mean value of H in the precession region, whereas the rms values of H is required to obtain $\Delta\nu$ from the measured value of ν_{24}.

Overlap from the (1,4) line introduces asymmetry into the (2,4) line, and makes ϕ_A and ϕ_B unequal. The error has been estimated from the observed differences between ϕ_A and ϕ_B. The rf magnetic field was kept constant by keeping the rf voltage at the feed point constant. Uncontrolled fluctuations of the rf voltage introduce only a random error; on the other hand the variation of impedance with frequency introduces a systematic error, which is, however, negligibly small.

Poor reception and a possible Doppler shift in transmission limited the accuracy with which our frequency standard could be adjusted to agree with WWV.

CONCLUSION

17. Final Result

From the foregoing, we arrive at the value

$$\Delta\nu(2S)=177\ 556.86\pm0.05 \text{ kc/sec.}$$

It is instructive to use this result to compute the ratio R defined in the introduction. The results of recent determinations of $\Delta\nu(1S)$ are 1 420 405.80±0.05 kc/sec[1] and 1 420 405.73±0.05 kc/sec[2]. Because the difference between these two values of $\Delta\nu(1S)$ does not affect R significantly, we use only the result of Kusch[2] to compute R and obtain

$$R_{\text{exp}}=\tfrac{1}{8}(1.000\ 034\ 6\pm0.000\ 000\ 3).$$

18. Discussion

Fermi[18] has derived a theoretical expression for the hfs of $^2S_{\frac{1}{2}}$ states:

$$\Delta\nu=(8\pi/3)[(2I+1)/I]\mu_0\mu_I\Psi^2(0)/h, \qquad (6)$$

where $\Psi(r)$ is the nonrelativistic Schrödinger wave function. By use of (6) a theoretical value of exactly $\frac{1}{8}$ is obtained for R.

Breit[3] has calculated relativistic correction factors for the hfs of $1S$ and $2S$ states from which Eq. (1) was derived. With $\alpha=1/(137.0365\pm0.0012)$ (HVI), we obtain

$$R_{\text{theor}}=\tfrac{1}{8}[1+(5/8)\alpha^2]=\tfrac{1}{8}(1.000\ 033\ 3).$$

There remains a discrepancy

$$\Delta R=R_{\text{exp}}-R_{\text{theor}}=\tfrac{1}{8}(13\pm3)\times10^{-7}.$$

It is not reasonable to attribute the discrepancy ΔR to nuclear-structure effects. For small values of r,

$$[\Psi_{2s}(r)/\Psi_{1s}(r)]^2=\tfrac{1}{8}[1-\tfrac{1}{4}(r/a_0)^2].$$

Recent experiments[19] indicate a proton radius of 1.0×10^{-13} cm. Thus, the effect of nuclear structure upon R is only of the order of one part in 10^{10}. Kroll[20] has suggested that ΔR arises from a quantum-electrodynamical effect of order α^3, which is being calculated by M. Mittleman.[21] Tentatively, we may write

$$R_{\text{theor}}=\tfrac{1}{8}[1+(5/8)\alpha^2+X\alpha^3],$$

where experimentally $X=3.4\pm0.8$.

ACKNOWLEDGMENTS

Credit is due Professor W. E. Lamb, Jr., for originally proposing this experiment. We are indebted to Professor N. M. Kroll and Dr. R. Novick for many helpful discussions. We wish to thank the members of the Columbia Radiation Laboratory for their continued assistance. Mr. S. Marcus assisted in taking and evaluating the final data.

APPENDIX A. STARK EFFECT

A rigorous calculation of the Stark shifts of the levels 1, 2, 3, and 4, which are produced by the coupling of the $2P$ states with $2S$ states through an external electrostatic field E, would begin with the setting up of the complete energy matrix in the $H=E=0$ representation. Diagonalization of this matrix would be more cumbersome than is justified here.

Our interest is in finding the Stark effect on the value of $\Delta\nu(2S)$ as it is determined in the present work. This is the same as the change in ν_{24} produced by an electrostatic field. This quantity $\delta\nu_{24}$ may be calculated by second-order perturbation theory if the electric perturbation ea_0E is much less than the magnetic perturbation μ_0H, that is, if

$$E\ (\text{in volts/cm})\ll H\ (\text{gauss}).$$

Since the $2\,^2P_{\frac{3}{2}}$ states are much farther removed from $2S$ than the $2\,^2P_{\frac{1}{2}}$ states, the Stark shift produced by the former is neglected here. Under these conditions it can be shown that ν_{24} is changed by an amount

$$\delta\nu_{24}=-3(a_0e/h)^2\{E^2[(8-5\Delta\nu/6)^{-1}-(8+\Delta\nu/6)^{-1}]+E_z^2[(8+\Delta\nu/6)^{-1}-(8+\Delta\nu/2)^{-1}]\},$$

where **H** is assumed to be in the z-direction. If E and E_z are given in volts/cm,

$$\delta\nu_{24}=-(0.88E^2+0.23E_z^2)\ \text{kc/sec}. \qquad (7)$$

The presence of E_z in Eq. (7) expresses the assumption that the z-direction is the preferred direction. It is to be noted, first, that Eq. (7) is not valid for $H=0$, and second, that the Stark effect gives an apparent value of $\Delta\nu(2S)$ that is lower than the true value.

A quantitative theory of the rf Stark effect, as it might occur in this experiment, is exceedingly complicated. It is certain, however, that in the presence of rf electric fields ν_{24} is decreased, and it is likely, at least for weak rf fields, that the rf Stark effect is proportional to the square of the rf amplitude.

APPENDIX B. FORMULA FOR THE DECAY LENGTH

The curves in Fig. 3 were computed from the formula

$$1/\lambda=(3/\alpha)^2\gamma(v/c^2)x^2\sum[A_i/(B_i^2+D^2)], \qquad (8)$$

where α is the fine-structure constant, $\gamma=6.26\times10^8$ sec^{-1} is the spontaneous decay rate of the $2P$ state, v is the velocity of the atom, $x=(3\mu_0H)/(2\Delta E)$, and $D=(3h\gamma)/(8\pi\Delta E)$.

TABLE IV. Values of A_i and B_i for the states α and β. The values of the y's and $\delta_\pm$ are given by Eqs. (164) to (167) and (201) in HIII.

State	i	A_i	B_i
	1	2	y_a-y_α
α	2	$1+\delta_-$	y_c-y_α
	3	$1-\delta_-$	$y_\alpha-y_f$
	1	2	y_d-y_β
β	2	$1-\delta_+$	y_b-y_β
	3	$1+\delta_+$	$y_\beta-y_e$

The meaning of A_i and B_i is given in Table IV. Equation (8) was derived from Eq. (2) of Sec. 3 and Eq. (76) of HII. The variation of matrix elements with H has been taken into account, but hfs has been neglected.

[18] E. Fermi, Z. Physik **60**, 320 (1930).
[19] R. Hofstadter and R. W. McAllister, Phys. Rev. **98**, 217 (1955).
[20] N. M. Kroll (private communication).
[21] *Note added in proof.*—It has been suggested that ΔR may also arise in part from a differential proton recoil correction to the hfs.